

Application of x-ray direct methods to surface reconstructions: The solution of projected superstructures

X. Torrelles and J. Rius

Institut de Ciència de Materials de Barcelona (C.S.I.C.), 08193 Bellaterra, Catalunya, Spain

F. Boscherini

Istituto Nazionale de Fisica Nucleare, Laboratori Nazionali di Frascati, P.O. Box 13, I-00044 Frascati (Roma), Italy

S. Heun and B. H. Mueller

Laboratorio TASC-INFM, Padriciano 99, 34012 Trieste, Italy

S. Ferrer and J. Alvarez

European Synchrotron Radiation Facility, Boîte Postale 220, 38043 Grenoble Cedex, France

C. Miravittles

Institut de Ciència de Materials de Barcelona (C.S.I.C.), 08193 Bellaterra, Catalunya, Spain

(Received 4 November 1997)

The projections of surface reconstructions are normally solved from the interatomic vectors found in two-dimensional Patterson maps computed with the intensities of the in-plane superstructure reflections. Since for difficult reconstructions this procedure is not trivial, an alternative automated one based on the “direct methods” sum function [Rius, Miravittles, and Allmann, *Acta Crystallogr.* **A52**, 634 (1996)] is shown. It has been applied successfully to the known $c(4 \times 2)$ reconstruction of Ge(001) and to the so-far unresolved $\text{In}_{0.04}\text{Ga}_{0.96}\text{As}$ (001) $p(4 \times 2)$ surface reconstruction. For this last system we propose a modification of one of the models previously proposed for GaAs(001) whose characteristic feature is the presence of dimers along the fourfold direction. [S0163-1829(98)50908-3]

Unlike most metal surfaces that only show relaxation, the majority of semiconductor surfaces reconstruct. One common mechanism for the reconstruction is the formation of dimers. Compared to the unreconstructed surface, a reconstructed surface shows a large surface unit cell and can therefore be described as a surface with a reduced number of lattice points but an increased number of basis atoms. If the reciprocal space vectors are expressed in terms of the reciprocal space basis $(\mathbf{b}_1, \mathbf{b}_2, \mathbf{b}_3)$ with \mathbf{b}_3 normal to the reconstructed surface, then this reduction of lattice points causes the appearance of fractional-order rods $[h, k, l_z]$. Since the present paper concerns the solution of projected superstructures, only rod values with the continuous coordinate l_z equal to zero will be considered. These values constitute the set of in-plane superstructure reflections (h, k) .

The difference function δ is defined as the difference between the projected superstructure ρ_p and the corresponding average function $\langle \rho_p \rangle$ obtained by averaging the electron density over the superstructure unit cell. It can be expressed in the form of a partial Fourier synthesis including only terms of the superstructure reflections

$$\delta(\mathbf{x}) = \frac{1}{S} \sum_{\mathbf{h}} |E(\mathbf{h})| \exp[i\varphi(\mathbf{h})] \exp(-2\pi\mathbf{h} \cdot \mathbf{x}), \quad (1)$$

and has the same symmetry as ρ_p (S = area of the surface unit cell).^{1,2} In most cases, its determination requires the solution of the superstructure ρ . Unfortunately, the phase val-

ues $\varphi(\mathbf{h})$ required for the computation of Eq. (1) are not available. Since δ contains positive and negative values, the power of conventional direct methods to find $\varphi(\mathbf{h})$ directly from the normalized structure factors $|E(\mathbf{h})|$ is weakened. One possible way of solving δ is through the direct interpretation of the two-dimensional (2D) difference Patterson-like functions $\delta P_0(x)$ (also called “surface autocorrelation functions”) as, e.g., the modulus synthesis^{1,2}

$$\delta P_0(\mathbf{x}) = \frac{1}{S} \sum_{\mathbf{h}} |E(\mathbf{h})| \exp(-i2\pi\mathbf{h} \cdot \mathbf{x}). \quad (2)$$

This is the procedure normally used for simple reconstructions. When the reconstruction involves a large number of atoms or when the interatomic peaks do not show up clearly in the Patterson map, an automated interpretation procedure like the “direct methods” sum function¹ is desirable. The direct methods sum function can be written in the form of the integral

$$S \int_S \delta P_0(\mathbf{x}) \delta P(\mathbf{x}, \Phi) d\mathbf{x}, \quad (3)$$

which measures the coincidence between the observed 2D difference Patterson-like function δP_0 and the calculated one $\delta P(\Phi)$ given in terms of the collectivity Φ of phases of the largest superstructure reflections. As was demonstrated in Ref. 2, the possibility of expressing the difference Patterson-

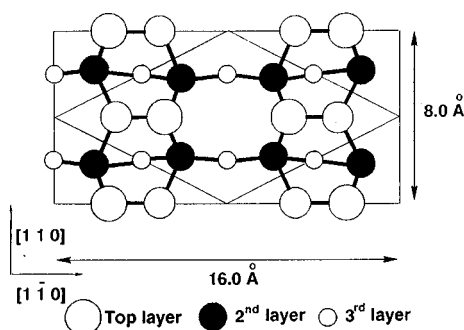


FIG. 1. Upper view of the Ge(001) $c(4 \times 2)$ reconstruction showing the dimers and the first (filled circles) and second sublayers.

like function as a function of Φ follows from the assumption that δ resembles its cube. Obviously, integral (3) will be a large positive quantity if the coincidence between observed and calculated difference Patterson functions is good. In practice, the starting random values of the phases $\varphi(\mathbf{h})$ in Φ are refined by maximizing the direct methods sum function with an extended tangent formula² (SUMF-TF) and minimizing $\sum_l |C_l(\Phi)|$ where l denotes the weakest superstructure reflections and $|C_l(\Phi)|$ the amplitudes of the δ^3 normalized structure factors. The refined values are then introduced in Eq. (1) to compute δ . For a detailed description of the method see Refs. 1 and 2.

The 3D version of this procedure has been already used to redetermine the superstructure of mineral “wernlandite” from high-quality x-ray diffraction data.² Here, the applicability of the SUMF-TF to solve the projections of two superstructures from the intensities of their in-plane superstructure reflections will be shown: (i) the already known Ge(001) $c(4 \times 2)$ surface reconstruction³ that is used as a preliminary test; (ii) the projection of the still unresolved $\text{In}_{0.04}\text{Ga}_{0.96}\text{As}$ (001) $p(4 \times 2)$ surface reconstruction. $\text{In}_{0.04}\text{Ga}_{0.96}\text{As}$ is lattice matched to ZnSe and therefore interesting for blue laser applications.^{4,5}

Both experiments were performed at the surface diffraction beamline of the European Synchrotron Radiation Facility.⁶ The energy for the Ge(001) $c(4 \times 2)$ experiment was 16 keV (fifth harmonic of the undulator) and for the $\text{In}_{0.04}\text{Ga}_{0.96}\text{As}$ (001) $p(4 \times 2)$ 18.4 keV (seventh harmonic). Both samples were installed in a UHV system coupled to a six-circle diffractometer operated in the z -axis mode.⁷

The capability of the SUMF-TF for solving projected superstructures was first checked using the experimental set of the Ge(001) $c(4 \times 2)$ reconstruction (Fig. 1),³ which consists of 46 nonequivalent in-plane reflections specific to the $c(4 \times 2)$ structure measured in one of the two existing domains at the surface. Half-order reflections common to the structures $c(4 \times 2)$ and $p(2 \times 1)$ were not considered. The intensities of the 46 in-plane superstructure reflections were normalized. The phases of the five reflections with the largest normalized intensities (E values) were refined using these E values and the E values of the six weakest reflections. The number of refined sets was 50 and the number of cycles for each set was six. As was shown in Ref. 2, the best solution is that which maximizes the integral (3). Figure 2 shows the δ map (with suppressed negative regions) computed with the

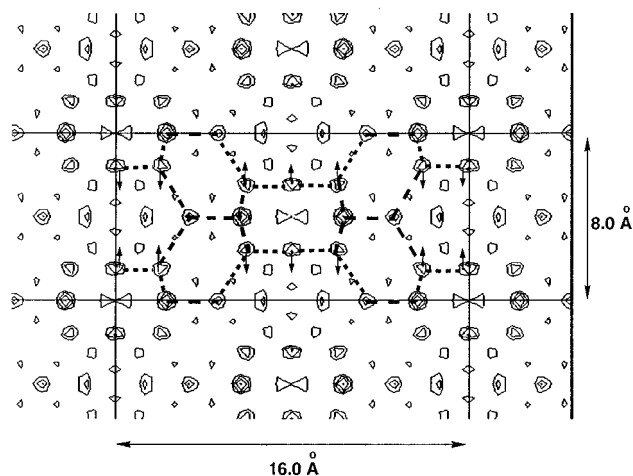


FIG. 2. $\delta(x,y)$ map of the Ge(001) $c(4 \times 2)$ reconstruction obtained from the phase refinement with the SUMF-TF using only part of the in-plane superstructure reflections (negative regions of the map are suppressed). To help the comparison with Fig. 1, most bonds involving the dimers and atoms of the first and second sublayers have been outlined. For the meaning of the arrows, see the text.

phase values of the best solution. Comparing Figs. 1 and 2 it is evident that the projection of the superstructure can be easily recognized from the δ map. However, some care is necessary, since, according to the definition of δ , certain peaks in δ must appear slightly shifted from the corresponding atomic position in ρ_p (see, for example, the arrows in Fig. 2).² One promising aspect of this first test is the viability of applying direct methods to partial data sets (at least for superstructures involving a reduced number of atoms).

The $\text{In}_{0.04}\text{Ga}_{0.96}\text{As}$ samples were grown by solid source molecular-beam epitaxy in a system that includes interconnected chambers for the growth of III-V and II-VI materials.^{8,9} GaAs buffer layers 500 nm thick were initially grown at 600 °C on semi-insulating GaAs (001) wafers. $\text{In}_{0.04}\text{Ga}_{0.96}\text{As}$ epilayers 2 μm thick were subsequently grown at 500 °C with a III/V beam pressure ratio of approximately 1:40, as determined from an ion gauge positioned at the sample location. The indium content was calibrated by means of photoluminescence spectroscopy,¹⁰ giving 0.046(2). In the growth conditions employed, the GaAs as well as the $\text{In}_{0.04}\text{Ga}_{0.96}\text{As}$ buffer layers exhibited a 2×4 surface reconstruction, as monitored *in situ* by means of reflection high-energy electron diffraction (RHEED). To protect the surface during transport, the samples were capped and cleaned by annealing up to 450 °C; during decapping *in situ* RHEED showed the surface symmetry to evolve from (2×4) to (4×2) , at which point annealing was stopped. The reciprocal space basis of the average structure was selected with \mathbf{b}_1 and \mathbf{b}_2 parallel to the $[1, -1, 0]$ and $[1, 1, 0]$ directions, respectively, and \mathbf{b}_3 perpendicular to the surface. Their magnitudes are $b_1 = b_2 = 2\pi/a$ ($a = 4.011$ Å) and $b_3 = 2\pi/a_0$ with a_0 (bulk constant) = 5.672 Å. The symmetry of the diffraction pattern is *mm*. Inspection of the diffraction pattern along \mathbf{b}_1 showed well-defined peaks at positions that are multiples of 0.25 indicating the existence of a fourfold reconstruction in this direction. *In situ* RHEED experiments

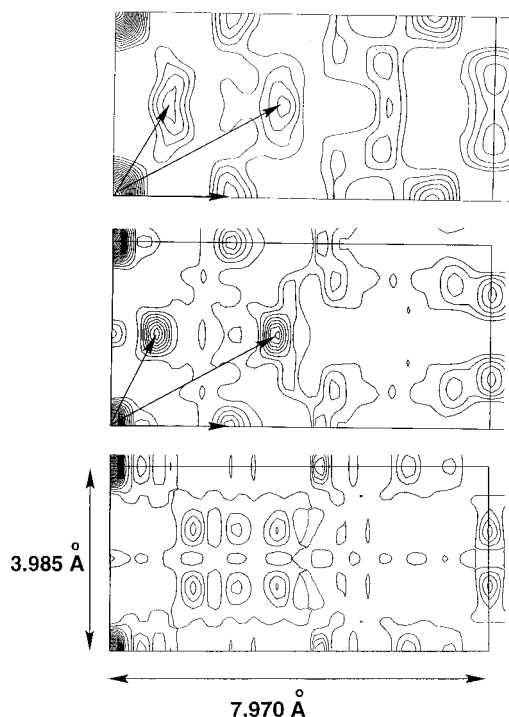


FIG. 3. (a) 2D Patterson function calculated with the measured intensities of the $\text{In}_{0.04}\text{Ga}_{0.96}\text{As}$ (001) in-plane superstructure reflections; (b) Patterson function map for the model by Skala *et al.* for GaAs(001) 4×2 ; (c) Patterson function for GaAs(001) $\beta 2(4\times 2)$. In (a) and (b) we show three similar interatomic vectors.

and an additional in-plane scan along $k = \frac{3}{2}$ using synchrotron radiation revealed that the half-order lines related to the two-fold periodicity in the \mathbf{b}_2 direction were too diffuse to be measured, which indicates the presence of strong disorder along this direction.¹¹ Consequently, the measured in-plane superstructure intensity data only contains reflections of the

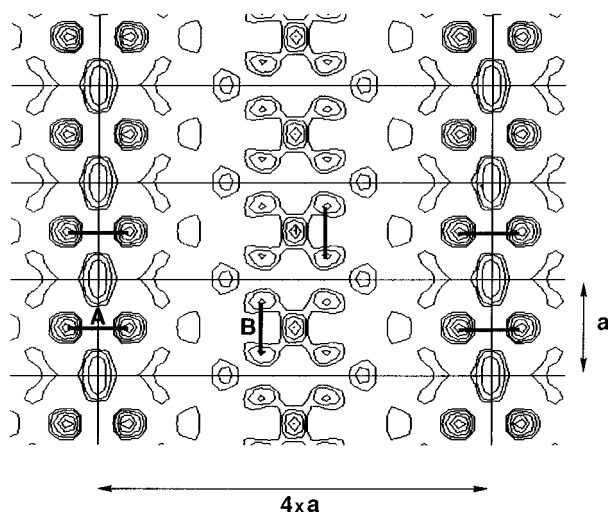


FIG. 4. $\delta(x,y)$ map of $\text{In}_{0.04}\text{Ga}_{0.96}\text{As}$ (001) $p(4\times 1)$ as obtained from the phase refinement with the SUMF-TF (negative regions of the map are suppressed). Lines A and B indicate the As and Ga dimers, respectively. Due to the half population of the Ga dimers, their peak strength is lower than for the As dimers.

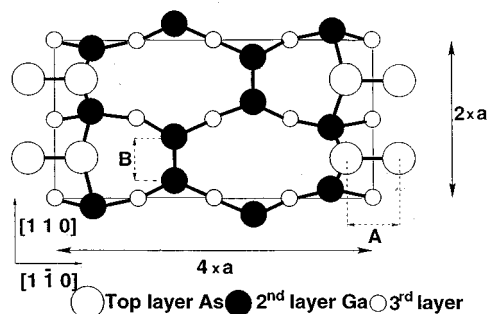


FIG. 5. Projected "ball and stick" model of the $p(4\times 2)$ unit cell derived from the δ map in Fig. 4, assuming a b glide mirror relating the Ga dimers ($P2mg$ symmetry).

type (h = "fractional," $k = 2n$) which can correspond either to a superstructure $p(4\times 2)$ averaged in the $[110]$ direction [hereafter denoted by $p(4\times 1)$], or to a superstructure $c(8\times 2)$ averaged in $[1,-1,0]$ and in $[1,1,0]$ to give the same $p(4\times 1)$ cell.¹² The angle of incidence of the x-rays to the surface was kept constant at 1° for all measurements. The in-plane diffraction data were collected at small values of the perpendicular momentum transfer ($I_z = 0.17$). Only one domain corresponding to the $p(4\times 2)$ orientation was formed after the sample preparation. A total of 151 in-plane fractional-order reflections were measured that reduced to 35 nonequivalent reflections with resolution lower than 1 \AA . At higher resolutions, the signal-to-noise ratio of the measured intensities was very poor and therefore they were disregarded.

The Patterson map computed with the in-plane superstructure reflections assuming pmm symmetry is given in Fig. 3(a); in Figs. 3(b) and 3(c) we show theoretical Patterson maps for two of the several models proposed in the literature for GaAs(001): the one by Skala *et al.*¹² and the so-called $\beta 2(4\times 2)$ model.¹³ Even though these models apply to GaAs surfaces it is reasonable to use them as a first approximation, given the low In concentration. It is quite clear from Fig. 3 that the model by Skala *et al.* has the highest resemblance to the experimental Patterson map, in particular, the experimental function shows the presence of a clear atomic correlation along \mathbf{b}_1 present only in the Skala *et al.* model and due to an As dimer. The main difference is the peak at $(0, 0.425)$ that, as shown later, is due to an In enrichment at site $\delta(1/2, 1/2)$.

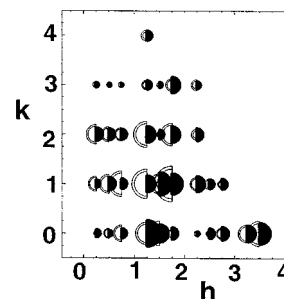


FIG. 6. Observed (outer empty semicircles) and calculated (filled semicircles) structure factors of the in-plane superstructure reflections of $\text{In}_{0.04}\text{Ga}_{0.96}\text{As}$ (001) $p(4\times 1)$. The error bars of the data are proportional to the area between outer and inner radii.

TABLE I. Fractional atomic coordinates (x, y) and anisotropic temperature coefficients (in \AA^2) for the model refined in the $p(4 \times 1)$ unit cell assuming the $P2mm$ symmetry. Column one indicates the type, number, and layer of the atom (topmost layer:1; bottom layer:4).

Atom	x	y	z	$B(x)$	$B(y)$
As-1:1	0.075(2)	$\frac{1}{2}$	-0.01(1)	5(2)	0
Ga-2:2	0.149(2)	-0.05(1)	-0.29(1)	0	0
Ga-3:2	0.339(2)	0.18(1)	-0.24(1)	4(2)	0
As-4:3	0	0	-0.50(1)	6(2)	2(2)
As-5:3	0.292(2)	0	-0.53(1)	5(2)	3(2)
As-6:3	$\frac{1}{2}$	0	-0.49(1)	5(2)	3(2)
Ga-7:4	0	$\frac{1}{2}$	-0.76(1)	0	0
Ga-8:4	0.259(2)	$\frac{1}{2}$	-0.79(1)	0	0
Ga-9:4	$\frac{1}{2}$	$\frac{1}{2}$	-0.72(1)	0	0

Due to the presence of elongated and poorly defined peaks along \mathbf{b}_2 , the direct interpretation of the map is not trivial. This represents an ideal case for solving the projection of the superstructure applying the SUMF-TF. The phases refined were those of the eight strongest superstructure reflections. The number of amplitudes actively used in the phase refinement was 21, i.e., 8 strong plus 13 weak E values. Since the total number available is 35, this represents 60% of the measured in-plane data. The number of sets of phases refined was 100, and they were ranked according to their respective figures of merit. The top solution is highly reproducible since all 25 highest-ranked sets gave the same solution. The δ Fourier map of the superstructure projection (averaged in \mathbf{b}_2) for the top solution is given in Fig. 4 and shows the following.

(a) Dimers form in the topmost layer (lines A); with reference to the Skala *et al.* model we propose them to be As dimers.

(b) Dimers are in the second layer (lines B); for the same reason as above we propose these to be Ga dimers. The two physically reasonable ways of placing the Ga dimers are (i) in a $p(4 \times 2)$ unit cell with a b glide plane relating the two Ga dimers in a zigzag manner, as depicted in Fig. 5 (the existence of this plane is compatible with the absence of

half-order peaks along \mathbf{b}_2); and (ii) in a $c(8 \times 2)$ unit cell with a mirror plane relating the two neighbor Ga dimers, as proposed in Ref. 12 on the basis of scanning tunneling microscopy images.

This model was confirmed, refining it with the in-plane data set as well as with the also measured (10), (01), and (11) bulk rods (155 additional observations). The number of refined variables was kept to a minimum (1 scaling factor, 16 positional parameters, 8 anisotropic in-plane temperature factor coefficients, and 1 occupational parameter). The atomic coordinates of this preliminary refinement are summarized in Table I [$R(F)=16\%$ for all data used in the refinement; $R(F)=30\%$ for the in-plane data only]. The temperature coefficients are only used to obtain information on the sites of the unit cell more affected by the disorder. Note the rather high error values given to them.

As for the position of In, we note that the δ Fourier map shows a strong and well-defined peak at $(1/2, 1/2)$, which we tentatively assign to an In enrichment at this site. In fact, the refinement of the occupancy factor for this atom site indicates a 30–50% In enrichment. Figure 6 shows graphically the results of the fit. The radii of the empty and filled semi-circles are proportional to the observed and calculated structure factors, respectively. The still rather high R value is due to the limited number of observations, which does not allow the introduction of the proper modeling of the disorder along both directions of the unit cell by taking into account (i) the partial substitution of Ga by In (4%) and (ii) the own disorder produced by the averaging of a $p(4 \times 2)$ unit cell to a $p(4 \times 1)$.

The refined in-plane distance between As-1:1 forming the dimer is close to 2.5 \AA . The strong displacement of Ga-2:2 in the \mathbf{b}_2 direction could be an indication for tilted As dimers. The refined projected distance between the dimerized Ga-3:2 atoms is also close to 2.5 \AA . As indicated before, this is a preliminary refinement performed to confirm the correctness of the δ map. A more complete and detailed one that also includes the fractional rods is in progress now, and will be published in due course.

Helpful discussions with L. Sorba and A. Franciosi are gratefully acknowledged.

¹J. Rius, Acta Crystallogr. **A49**, 406 (1993).

²J. Rius, C. Miravittles, and R. Allman, Acta Crystallogr. **A52**, 634 (1996).

³S. Ferrer, X. Torrelles, V. H. Etgens, H. A. van der Vegt, and P. Fajardo, Phys. Rev. Lett. **75**, 1771 (1995).

⁴S. Heun, J. J. Paggel, L. Sorba, S. Rubini, A. Franciosi, J.-M. Bonard, and J. D. Ganière, Appl. Phys. Lett. **70**, 237 (1997).

⁵S. Heun, J. J. Paggel, L. Sorba, S. Rubini, A. Franciosi, J.-M. Bonard, and J. D. Ganière, J. Vac. Sci. Technol. B **15**, 1279 (1997).

⁶S. Ferrer and F. Comin, Rev. Sci. Instrum. **66**, 1674 (1995).

⁷M. Lohmeier and E. Vlieg, J. Appl. Crystallogr. **26**, 706 (1993).

⁸A. Bonani, L. Vanzetti, L. Sorba, A. Franciosi, M. Lomascio, P. Prete, and R. Cingolani, Appl. Phys. Lett. **66**, 1092 (1995).

⁹R. Nicolani, L. Vanzetti, Guido Mula, G. Bratina, L. Sorba, A. Franciosi, M. Peressi, S. Baroni, R. Resta, A. Baldereschi, J. E. Angelo, and W. W. Gerberich, Phys. Rev. Lett. **72**, 294 (1994).

¹⁰S. Paul, J. B. Roy, and P. K. Basu, J. Appl. Phys. **69**, 827 (1991).

¹¹M. Sauvage-Simkin, Y. Garreau, R. Pinchaux, M. B. Veron, J. P. Landesman, and J. Nagle, Phys. Rev. Lett. **75**, 3485 (1995).

¹²S. L. Skala, J. S. Hubacek, J. R. Tucker, J. W. Lyding, S. T. Chou, and K. Y. Cheng, Phys. Rev. B **48**, 9138 (1993).

¹³J. E. Northrup and S. Froyen, Phys. Rev. B **50**, 2015 (1994).